Carbohydrate Polymers 113 (2014) 471–479

Contents lists available at ScienceDirect

Carbohydrate Polymers

journal homepage: www.elsevier.com/locate/carbpol

Polysaccharide-based materials and their adsorption properties in aqueous solution

Leila Dehabadi, Lee D. Wilson*

Department of Chemistry, University of Saskatchewan, 110 Science Place, Saskatoon, Saskatchewan, Canada S7N 5C9

ARTICLE INFO

Article history:
Received 18 December 2013
Received in revised form 20 June 2014
Accepted 21 June 2014
Available online 10 July 2014

Keywords:
Polysaccharide
Synthesis
Characterization
Copolymer
Adsorption

ABSTRACT

Polysaccharides (PS) of cellulose, soluble, corn- and maize-derived starches with variable amylose/amylopectin content were cross-linked with epichlorohydrin (EPI) to form polymeric adsorbents. The properties of the cross-linked PS–EPI materials were prepared by varying the synthesis conditions (nature of polysaccharide, temperature, and reagent ratios) to afford network polymer materials with tunable properties. The optimized polymers were obtained at a reaction temperature (50–54 °C) according their yield were characterized using spectroscopic (IR and NMR) methods, and thermal gravimetric analysis (TGA). The textural and adsorptive properties of the polymers were evaluated using nitrogen gas and dye-based methods using *p*-nitrophenol. Solvent uptake, nitrogen adsorption, and aqueous dye sorption show that the amylose and amylopectin content in the PS–EPI copolymers display a complex relationship with their physicochemical properties. Polymers with greater cross-linking did not show incremental changes in water or dye uptake. Structural variation of the polysaccharide (i.e. branching, molecular weight, and relative amylopectin/amylose content) contributed to the sorption properties by modifying their textural properties and surface chemistry.

1. Introduction

Polysaccharides such as starch and cellulose from plant sources are relatively abundant, naturally occurring, nontoxic, inexpensive and economically important biomaterials. They are amenable to chemical modification which make them especially attractive biomaterial platforms to produce value-added materials in technologies such as in drug delivery (Hamdi, Ponchel, & Duchêne, 2001; Onofre & Wang, 2010; Sandra, 2009), biomedical devices (Marques, Reis, & Hunt, 2002), tissue engineering scaffolds (Gomes, Ribeiro, Malafaya, Reis, & Cunha, 2001), dispersions (da Sil Va, Oliveira, & Rao, 1997), waste water treatment (Crini, 2005) and bio-refineries (Kamm & Kamm, 2004).

Starch and cellulose are abundant plant-based biopolymers, where the former serves as the plant's main energy reserve while the latter provides structural stability to plant cell walls (Scheller & Conrad, 2005). Starch may occur as granules (small compact form of starch molecules) which are composed mainly of two biopolymers, where the main component is amylopectin (70–80%), a branched polymer comprised of α-1,4-linked glucose units with α-1,6 branching links. The secondary component is amylose, a linear polymer consisting mainly of α-1,4-linked D-glucose units (Copeland, Blazek, Salman, & Tang, 2009; Kubo et al., 2010; Richardson & Gorton, 2003; Varum & Smidsrod, 2005). X-ray structural analysis of starch granules indicates a model of repeating amorphous and crystalline domains (Varum & Smidsrod, 2005). The crystalline domains of starch are associated with amylopectin while the amorphous regions are associated with amylose interspersed with amylopectin (Singh, Singh, Kaur, Singh Sodhi, & Singh Gill, 2003). By comparison, cellulose is much more crystalline in nature due to its β-1,4 linked D-glucose units arranged in a linear chain with no coiling or branching (Varum & Smidsrod, 2005). These biopolymer components adopt a relatively linear and rigid conformation where the monomer units undergo extensive intramolecular and intermolecular H-bonding (Richardson & Gorton, 2003).

The tertiary structure of starch and cellulose impact their physicochemical properties. For example, the relative ease that cellulose chains form stabilizing intra- and intermolecular interactions result in a self-assembled material with high tensile strength and relatively low solubility in water and many organic solvents. Such properties that contribute to its suitable function as a plant cell wall structural component but limit its industrial use due to material processing challenges (Richardson & Gorton, 2003). On the other hand, the variable crystalline properties of starch granules due to the amylose and amylopectin content affect its structure and physicochemical properties. As in the case of

* Corresponding author. Tel.: +1 306 966 2961; fax: +1 306 966 4730.
E-mail address: lee.wilson@usask.ca (L.D. Wilson).

http://dx.doi.org/10.1016/j.carbpol.2014.06.083
0144-8617/

cellulose, the crystalline domains of starch makes it less soluble in water but the presence of the amorphous regions impart lower structural rigidity and greater water solubility. This variability affinity of such biopolymers to water is useful in the food industry for improving food texture but may attenuate the sorption properties with xenobiotics due to competitive water sorption in aquatic environments (Delval, Crini, Bertini, Filiatre, & Torri, 2005). Mixed biopolymers of starch may limit a detailed understanding of their structure and properties but such materials may display unique physicochemical properties that are nonlinear with respect to their composition. For example, starch with high amylose content is commonly associated with high viscosity due to increased interactions and entanglement of the linear amylose chains (Copeland et al., 2009). Enhanced interaction between amylose chains is relevant for preparing starch-based derivatives with high thermal and mechanical stability (Xie et al., 2009). Starch with high amylopectin content favors swelling whereas starch with high amylose content display decreased swelling capacity (Copeland et al., 2009; Sasaki & Matsuki, 1998; Tester & Morrison, 1990). Swelling is a property closely associated with expansion of the polymer network and is important in drug delivery or for entrapment of guest molecules of a suitable size. Therefore, materials with well-defined swelling properties are important in sorption-based applications. In a recent study, Kyzas, Bikiaris, and Lazaridis (2008) demonstrated that sorbents that undergo pre-swelling exhibit rapid dye adsorption.

To expand the range of applications of starch and cellulose, cross-linking is a versatile strategy that affords materials with tunable mechanical and chemical properties (Ayoub & Rizvi, 2009; Crini, 2005; Delval et al., 2005; Hamdi et al., 2001; Kaur, Ariffin, Bhat, & Karim, 2012; Onofre & Wang, 2010). The cross-linker introduces intermolecular bridges between biopolymer units which may alter the overall textural properties and surface chemistry of the polymer framework. For example, Ghosh Dastidar and Netravali (2013) cross-linked waxy maize starch to obtain an environmentally friendly resin that has improved toughness and water resistance than native starch. Hamdi et al. (2001) cross-linked soluble starch to form microspheres with controlled particles with narrow size distribution for drug delivery applications. The physicochemical properties of the polymers are varied by the reaction parameters (e.g. temperature, solvent, and prepolymer composition) (Ayoub & Rizvi, 2009). For example, Ashish, Khanderao, and Deelip (2013) employed high amylose starch to form biodegradable implants for sustained drug delivery. Kaur et al. (2012) studied the effects of cross-linker content on the physicochemical properties of starch and attributed their observations to cross-linking of the starch polymer chains. Onofre and Wang (2010) used cross-linked starch with variable amylose/amylopectin content to study the rates of sustained drug release and reported its influence on the degree of cross-linking.

In this study, starch with variable amylose and amylopectin content along with cellulose were modified by chemical cross-linking with epichlorohydrin at variable reaction conditions. The resulting polysaccharide-epichlorohydrin (PS–EPI) copolymers were studied by evaluating their sorptive uptake properties in aqueous solutions with a model organic dye adsorbate (*p*-nitrophenol; PNP). The results of this systematic study will contribute to a greater understanding of the relationship of the sorption properties and structure of such copolymer materials in aqueous solutions.

2. Experimental

2.1. Preparation of PS–EPI copolymers

Different sources of starch (corn, maize, high amylose, high amylopectin), cellulose and epichlorohydrin were obtained from Sigma–Aldrich (Oakville, ON, Canada) and used as received. The synthesis of starch–epichlorohydrin copolymer materials employed a modified procedure are described elsewhere (Pratt, Wilson, Kozinski, & Mohart, 2010). Briefly, an aqueous solution of NaOH (2 M) was used to dissolve and ionize the polysaccharide hydroxyl groups prior to the addition of variable amounts of epicholorohydrin (EPI) to produce cross-linked polymers. The effect of temperature on the cross-linking reaction was evaluated at 40, 50, 60 and 70 °C.

2.2. Characterization of PS–EPI copolymers

The products were characterized using ^{13}C solid NMR spectroscopy with a wide-bore (89 mm) 8.6 T Oxford superconducting magnet system equipped with a 4 mm CP-MAS (cross polarization with magic angle spinning) solids probe. Operating parameters were controlled using an Avance DRX360 console and workstation running TopSpin 1.3 (Bruker Bio Spin Corp; Billerica, MA, USA). Standard pulse programs utilized were included in the TopSpin 1.3 software. Samples were packed in 4 mm outer diameter zirconium oxide rotors capped with Teflon MAS rotor caps. Acquisition was carried out using MAS at a rotational speed of 5 kHz, 2-s recycle delay and 750 μs cross polarization time. The chemical shift of adamantane (δ = 38.6 ppm) was used as an internal shift reference.

Fourier transform infrared (FTIR) spectra were obtained with a BIO-RAD FTS-40 spectrophotometer operating in diffuse reflectance mode. Multiple scans were obtained with a 4 cm^{-1} resolution and corrected against spectroscopic grade KBr background as the sample matrix over the spectral range of 400–4000 cm^{-1}. Thermogravimetry analysis (TGA) was performed using a TGA Q50 (New Castle, DE) operated at a heating rate of 5 °C min^{-1} up to a maximum temperature of 500 °C under a N_2 (carrier gas) atmosphere.

2.3. Solvent swelling properties of copolymer materials

The swelling properties of the sorbent materials were studied by use of approximately 40 mg of material was equilibrated in 6 ml of solvent (either Millipore water or neat ethanol for 48 h). The weight of hydrated polymer (w_s) was determined after tamping dry with filter paper by weighing, and then drying in an oven at 60 °C for 12 h to a constant dry weight (w_d). The swelling ratio was calculated using the following Eq. (1):

$$S_w = \frac{w_s - w_d}{w_d} \times 100\% \quad (1)$$

2.4. Dye adsorption studies

The textural properties were evaluated using nitrogen adsorption and a dye-based sorption method with UV–vis detection. Aqueous dye solutions of *p*-nitrophenol (PNP) were prepared at pH 6, below the pK_a value (7.14) of PNP (Mohamed, Wilson, & Headley, 2010; Mohamed, Wilson, Headley, & Peru, 2011). Approximately 20 mg of the powdered and sieved (40 mesh) copolymers were mixed in 10 ml of solution containing PNP at variable concentration (0.1–25 mM) in 10 mM potassium phosphate monobasic buffer solution (pH 6) in 4 dram glass vials. The vials were sealed with parafilm between the cap and the glass bottle, followed by equilibration on a horizontal mechanical shaker (Poly Science, Dual Action Shaker) for 24 h at 180 rpm. The samples were then centrifuged (Precision Micro-Semi Micro Centricone, Precision Scientific Co.) at 1800 rpm for 30 min. The UV–vis absorbance of PNP in the supernatant solutions was measured at λ_{max} = 318 nm using a Varian CARY 100 double beam spectrophotometer at room temperature (295 ± 0.5 K). An absorbance calibration curve was obtained from standard solutions of PNP and the molar absorptivity of PNP

Table 1
Product yield (%) for copolymers containing soluble starch–EPI at various cross-linking ratios and reaction temperature (°C).

Copolymer ID code[a]	Mole ratio (PS–EPI)	Polysaccharide composition	Yield (%) 40–45 °C	Yield (%) 50–54 °C	Yield (%) 60–64 °C	Yield (%) 70–75 °C
SSE1	Low (1:2)	~50% (AM/AP)	86	98	66	62
SSE2	Medium (1:3.6)	~50% (AM/AP)	52	63	48	49
SSE3	High (1:5.4)	~50% (AM/AP)	56	71	69	37

[a] Numerical descriptors in the ID code refer to the different mole ratios of PS–EPI, as follows: 1 = low (1:2 mole ratio); 2 = medium (1:3.6 mole ratio); and 3 = high (1:5.4 mole ratio).

Table 2
Product yield (%) for PS–EPI polymers prepared at 50–54 °C.

PS–EPI copolymer	Polysaccharide composition	Copolymer ID code[a]	Yield (%) 50–54 °C
Corn starch–EPI (low)	(73% AP)	CSE-1	95
Corn starch–EPI (medium)	(73% AP)	CSE-2	53
Corn starch–EPI (high)	(73% AP)	CSE-3	56
Maize starch–EPI (low)	(98% AP)	MSE-1	71
Maize starch–EPI (medium)	(98% AP)	MSE-2	51
Maize starch–EPI (high)	(98% AP)	MSE-3	45
Low cellulose–EPI (low)	100%	CE-1	58
Cellulose–EPI (medium)	100%	CE-2	42
Cellulose–EPI (high)	100%	CE-3	45
High amylose corn-based (low)	(98% AM)	AMCE-1	77
High amylose corn-based (medium)	(98% AM)	AMCE-2	36
High amylose corn-based (high)	(98% AM)	AMCE-3	51

[a] Refer to footnotes in Table 1 for ID Code descriptors.

($\varepsilon = 9495\ M^{-1}\ cm^{-1}$) was determined using the Beer–Lambert relation. The equilibrium concentration (C_e) of PNP in the supernatant solutions was determined and the sorptive uptake (Q_e) of the sorbent material was calculated using Eq. (2), where V is the volume of solution, C_0 is the initial stock concentration (mM), and m is the mass of sorbent.

$$Q_e = \frac{C_0 - C_e}{m} \times V \quad (2)$$

The sorptive uptake (%P) of PNP from aqueous solution was calculated using Eq. (3).

$$\%P = \frac{C_0 - C_e}{C_0} \times 100\% \quad (3)$$

Nitrogen adsorption measurements were obtained using a Micromeritics ASAP 2020 (Norcross, GA) to obtain the surface area and pore structure properties. The surface area was calculated from the adsorption isotherm (Copeland et al., 2009) and the micropore surface area was determined using the de Boer t-plot method (Broekhoff & De Boer, 1968).

3. Results and discussion

3.1. Copolymer synthesis

As indicated above, the molecular structure of native starch and various other biopolymers can be modified by cross-linking with an appropriate linker unit such as epichlorohydrin (Ayoub & Rizvi, 2009; Delval et al., 2005; Hamdi et al., 2001; Onofre & Wang, 2010). Scheme 1 illustrates a generalized cross-linking reaction between epichlorohydrin (EPI) a linear polysaccharide; however, cross-linking between EPI with starch or cellulose occurs at either the secondary and primary hydroxyl groups. The PS -EPI copolymers were prepared at low, medium, and high reactant mole ratios (i.e. 1:2, 1:3.6 and 1:5.4). The temperature conditions for the cross-linking reaction were varied to determine the optimal cross-linking temperature conditions for polymer synthesis. The cross-linking of starch with epichlorohydrin afforded variable yields (50–98%) as shown in Tables 1 and 2. In Table 1, the greatest yield was obtained with the 1:2 starch-EPI mole ratios and at 50–54 °C synthesis conditions and it should be noted that the PS–EPI copolymer products are generally water insoluble. The yields obtained herein are comparable to values (75–95%) reported by Ashish et al. (2013), where high amylose starch was cross-linked with epicholorohydrin at 50 °C (cf. Table 1). The yield variability was attributed to the differences in type of polysaccharide, stirring rate, reagent concentrations, and reaction time. Ashish et al. (2013) used high amylose starch which is known to favor cross-linking reactions. In this study, different types of starch were used with amylose/amylopectin (AM/AP) with variable weight ratios (w/w %) to evaluate the effects of composition and branching on the polymer properties. The following PS systems were employed: soluble starch (50% AM/AP), corn starch (73% AP/27% AM), maize starch (98% AP), and cellulose to evaluate the effect of PS structural rigidity.

3.2. FT-IR spectroscopy

The IR spectra of starch and some selected representative copolymers are shown in Fig. 1. Additional IR results of other systems are provided in the Supporting information (cf. Fig. S1). The relative similarity of the IR spectra of starch and its cross-linked

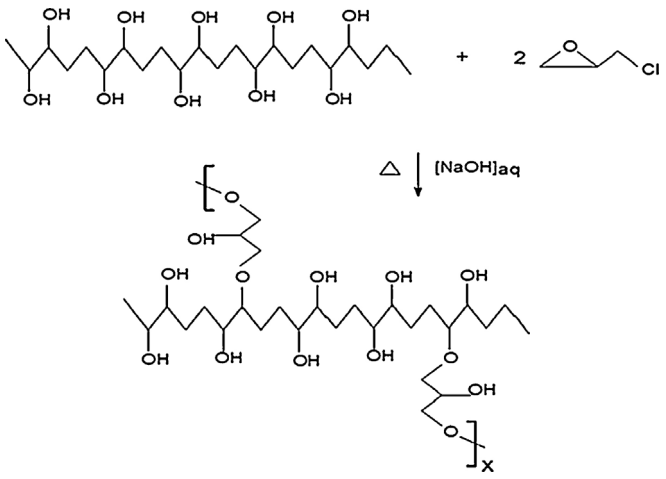

Scheme 1. Generalized cross-linking reaction between epichlorohydrin (EPI) with selected hydroxyl groups of a linear polysaccharide (PS).

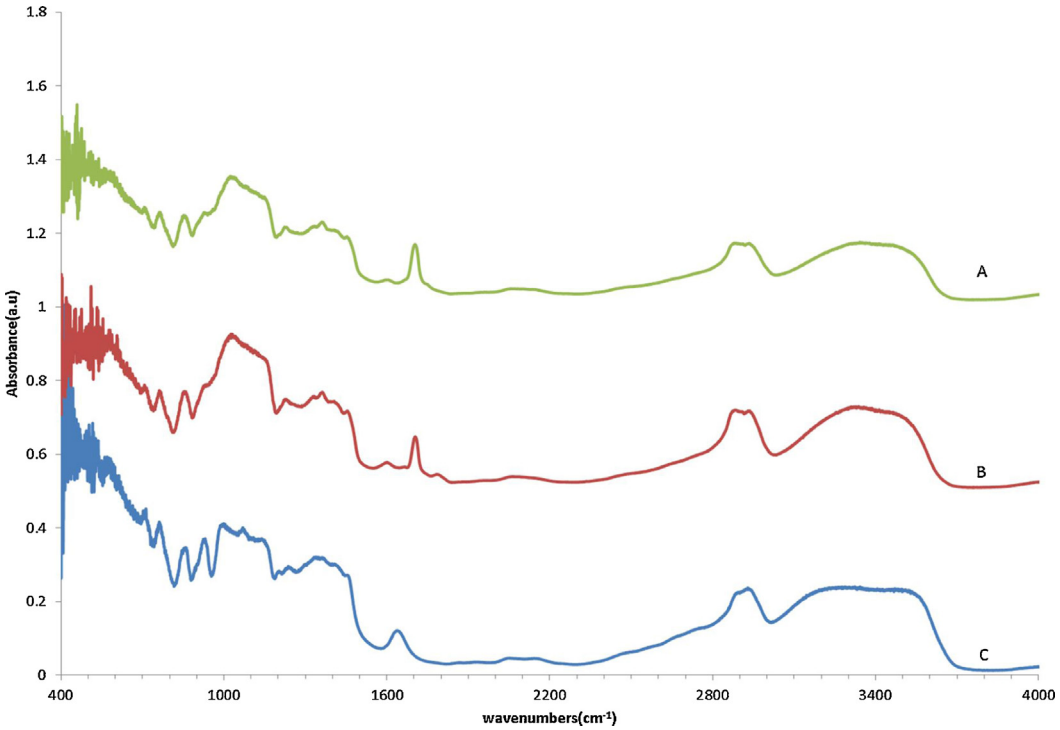

Fig. 1. FT-IR spectra of starch and its PS–EPI copolymers: (A) SSE-1 synthesized at 60–65 °C, (B) SSE-1 synthesized at 50–54 °C, and (C) unmodified starch.

forms support that the primary structure of the polysaccharide was preserved during copolymer formation, as anticipated. The spectral frequencies are in agreement with those reported elsewhere (Crini, 2005) and the following characteristic IR bands are observed: O—H stretching ~3400 cm^{-1}, C—H stretching ~2900 cm^{-1}, and C—C stretching ~1600 cm^{-1} with relatively similar spectral frequencies among the various copolymers prepared herein (Crini, 2005). The characteristic ring vibrations and the anomeric C—H deformation bands are observed between 900 and 550 cm^{-1}. Also, the broadening of bands in the range of 900 and 1400 cm^{-1} are attributed to cross-linking with epichlorohydrin (Delval, Vebrel, Morcellet, & Crini, 2000).

3.3. ^{13}C NMR spectroscopy

The polymeric materials have limited solubility in various organic solvents such as DMSO. Therefore, NMR spectra were obtained for selected samples in the solid state using CP-MAS NMR methods, as shown in Fig. 2. Each glucose monomer of starch contains six C atoms and the spectrum shows four broad ^{13}C NMR lines between 60 and 110 ppm with some overlapping of the various carbon signatures, as observed for amylose-based copolymers (Pratt et al., 2010). The results in Fig. 2 shows intense signals at 72.9, 71.4, 70.0, 63.6 and 61.7 ppm as well as a lower intensity signal at 100.5 ppm agree with other reports (Delval et al., 2000; Varum & Smidsrod, 2005; Šimkovic, Laszlo, & Thompson (1996)). There are four ^{13}C signatures for starch which appear at 100 ppm (anomeric carbon C1), 84 ppm (C4), 70 ppm (C2, C3, and C5), and 61 ppm (C6). A comparison of the spectra for the cross-linked polymers indicate greater line broadening relative to starch, and this is understood according the reduced chain dynamics (longer correlation times) of the polysaccharide upon cross-linking, as reported in a previous study of cycloamylose polymers cross-linked with epichlorohydrin (Delval et al., 2005; Pratt et al., 2010).

3.4. Thermogravimetry analysis (TGA)

TGA is a useful method for the quantitative characterization of material composition since it provides a measure of the weight loss due to decomposition, oxidation, or loss of volatile materials, and provides estimates of the relative composition (Pratt et al., 2010; Singh et al., 2003). In this study, TGA results are presented as a first derivative of mass loss with temperature against temperature (DTG plot) to provide information on the decomposition temperature and degree of cross-linking of the polymer materials. A greater degree of cross-linking for amylose-based materials is expected to increase the overall thermal stability of such polymers (Pratt et al., 2010). The DTG curves for starch, cellulose and selected polymers with EPI are shown in Fig. 3. The thermal decomposition of these materials occurs over the 200–400 °C range; whereas, DTG results for the "as-received" starch and cellulose show decomposition at ~290 and ~330 °C (cf. Fig. 2A and B). These temperature values agree with reported literature values of 280 °C for high amylose corn starch (Tian et al., 2013) and 330–334 °C reported for cellulose derived from corn cobs (Azubuike & Okhamafe, 2012). Cross-linking of these prepolymers with EPI results in PS–EPI copolymers with higher decomposition temperatures, providing further support that such materials display greater thermal stability. The polysaccharide materials display an average decomposition temperature of 364 ± 2 °C. The difference in thermal stability is evident for starch materials since the starch–EPI polymers display higher decomposition temperatures (~+70 °C), as compared to cellulose–EPI copolymers (~+15 °C). In Fig. 2C, MSE-1 contains ~98% amylopectin and showed the highest DTG intensity at 364 °C. Pratt et al. (2010) used DTG peak areas to estimate the polymer composition and the degree of cross-linking. In this case, no general trends can be gleaned from DTG intensity results that relate to the AM, AP, or content of EPI of the polymers. The degree of EPI cross-linking is affected by other factors such as steric effects due to branching of the polysaccharide (e.g. AP vs. AM) and framework

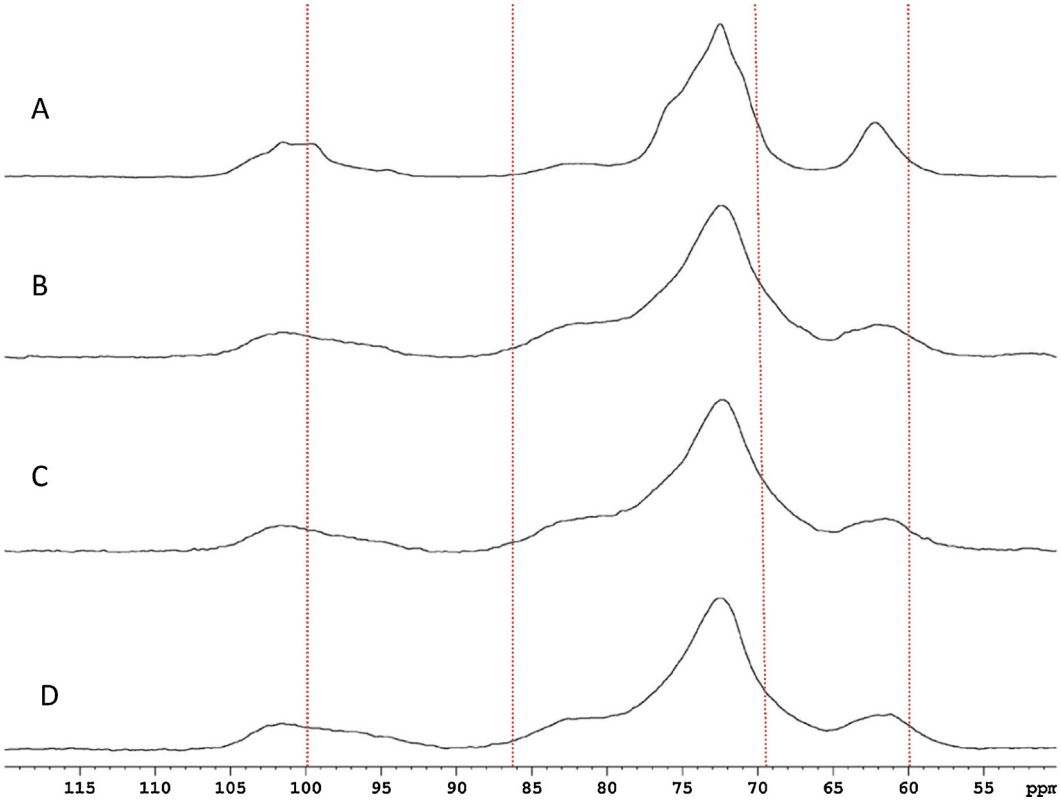

Fig. 2. Solid state ^{13}C CP-MAS NMR spectra of maize starch and selected PS–EPI copolymers at 295 K: (A) MSE, (B) MSE-1, (C) MSE-2, and (D) MSE-3.

structural effects depending on the nature of the polysaccharide and cross-linker. A closer inspection of the DTG curves show that they can be best modeled by a sum of three Gaussian functions centered at 270, 320 and 360 °C (refer to Supporting Information; Fig. S1). Apart from the decomposition temperatures of the PS (270 °C) and the PS–EPI framework (360 °C), there is another thermal event at 320 °C. A TG/mass spectrometry study of starch-EPI thermal decomposition showed that other pathways, aside from polymer dehydration, as the main route of starch–EPI decomposition which yield secondary degradation products (Šimkovic & Jakab, 2001). The presence of other thermal events in the DTG plots can be used to infer the presence of different types of cross-linked materials. Table 3 summarizes the relative peak area (%) for the various thermal events of each of the polymer. Using the peak area under the 360 °C event in panel C, it can be related to the degree of cross-linking in descending order: AMCSE1 > SSE1 ≈ CSE1 > MSE1.

Table 3
TGA results for PS–EPI copolymers prepared at 50–54 °C.

Copolymer ID code[b]	Peak area (270 °C)	Peak area (320 °C)	Peak area (360 °C)
CSE-1	25%	21%	53%
CSE-2	30%	39%	30%
CSE-3[a]	21%	9%	69%
MSE-1	12%	57%	30%
MSE-2	14%	57%	28%
MSE-3[a]	11%	27%	61%
AMCSE-1	31%	14%	55%
AMCSE-2	31%	14%	55%
AMCSE-3[a]	15%	32%	52%
SSE-1	29%	16%	54%
SSE-2	39%	10%	51%
SSE-3[a]	16%	27%	58%

[a] Areas under the curve were taken from convolution of three Gaussians but the fit was not optimal.
[b] The fitting details found in supporting information.

This trend is consistent with the relative reactivity of such PS materials with EPI. AMCSE is a linear PS allowing for ease of accessibility of hydroxyl groups to react with EPI, whereas; MSE is a branched PS, which may present some steric accessibility of its hydroxyl groups for EPI cross-linking. The relative amount of cross-linking of EPI is estimated from the integrated area of the respective thermal event (at 360 °C) corresponding to copolymer decomposition profile. In panel D, intermediate ratios of EPI were used and the results show a similar trend as in panel C. However, by increasing the amounts of EPI (panel E), the TGA results can no longer be modeled by a simple sum of three Gaussian functions. Instead, the DTG results can be modeled by a minimum of six Gaussian components (cf. Supporting Information; Fig. S2) and reveals that cross-linking has resulted in copolymers with heterogeneous domains of intermediate and higher levels of cross-linking.

3.5. Equilibrium solvent swelling properties

The equilibrium swelling of the unmodified polysaccharides and respective cross-linked polymers provide an indication of the relative uptake of the solvent (i.e. water or ethanol) at ambient conditions. Swelling is an important property to measure when assessing the potential of new adsorbent materials since solvent uptake plays a role in the adsorption process, as evidenced by the elementary kinetic steps (e.g. film diffusion, intraparticle diffusion, surface adsorption). For example, Kyzas et al. (2008) reported the relationship of swelling and dye sorption properties of chitosan derivatives. They described the role of pre-swelling of the adsorbents prior to dye adsorption in aqueous solution and how it affects the rate of the adsorption process. The swelling behavior of the adsorbent materials in water and ethanol [S_w and S_e; Eq. (1)] are presented in Table 4. It is noted that the AMCSE copolymers have a greater adsorption capacity for water relative to ethanol, whereas the MSE polymers display the opposite behavior. The PS–EPI

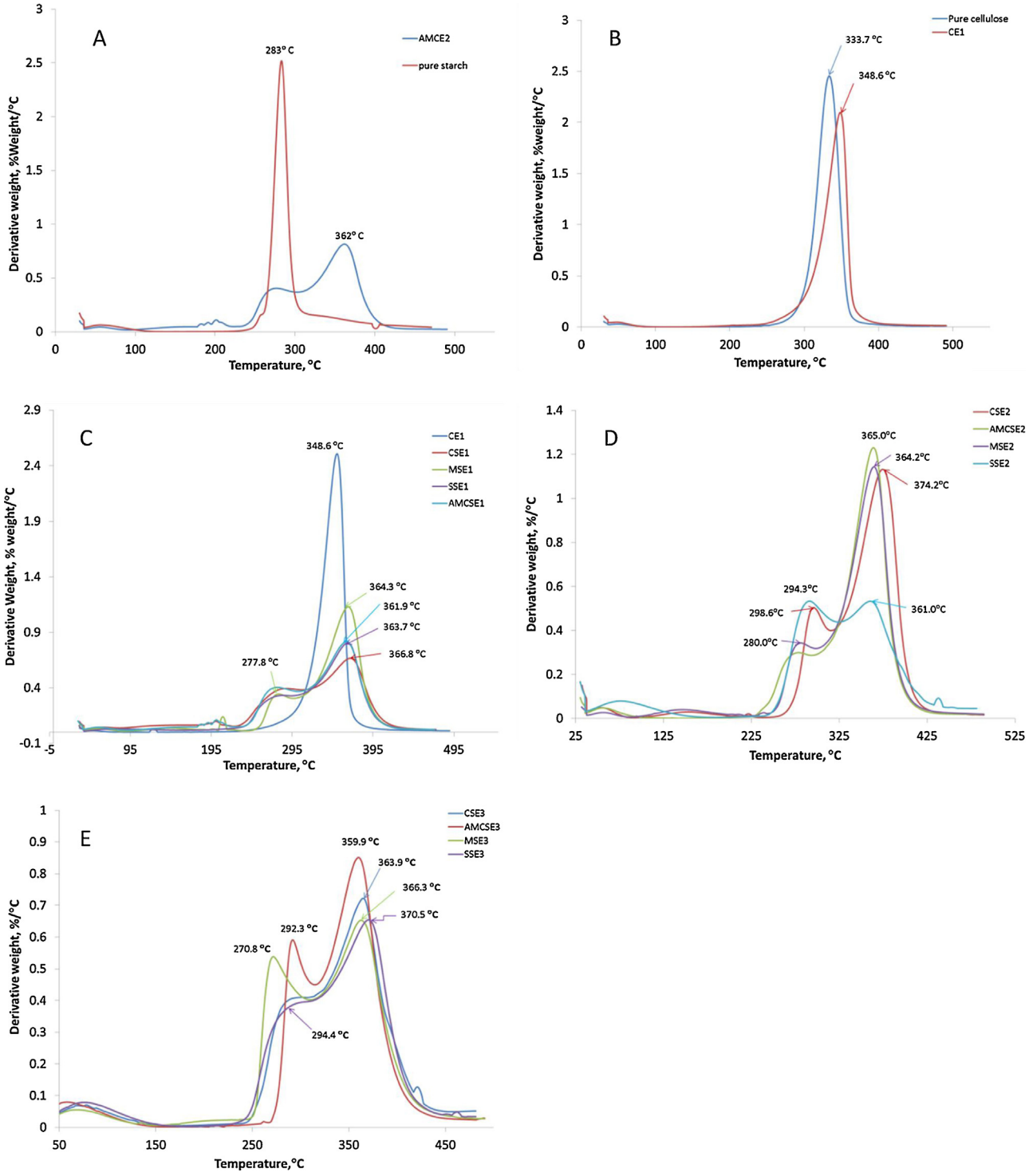

Fig. 3. First derivative plots of (A) pure starch and starch–EPI copolymer; (B) pure cellulose and cellulose–EPI copolymer and (C–E) various PS–EPI copolymers.

polymers display a greater preference for the uptake of water over ethanol. The occurrence of selective solvent uptake by the copolymers depends on several factors: (i) textural properties (i.e. pore size, pore volume, and surface area), and (ii) surface chemistry of the polymer framework according to the relative accessibility of hydroxyl groups of the sorbent. Polymers with a pore size less than 4 Å will preferentially adsorb water (2.8 Å) due to steric exclusion effects (Sasaki & Matsuki, 1998). In contrast, copolymers with a pore size exceeding 4 Å can retain either species since ethanol has a greater size (4.6 Å) (Sasaki & Matsuki, 1998). Since the polymers prepared in this study have similar pore size in the range of ~21–28 Å, steric effects are not anticipated. Solvent selective adsorption may occur depending on the surface chemistry of the framework. In cases where the surface accessibility of hydroxyl groups is variable, the surface chemistry may govern the adsorptive interactions, as evidenced by the variable swelling capacity of the different copolymers. When the AM units are self-assembled and aligned within the polymer structure, the probability of AM cross-linking with another AM is high (cf. Scheme 2). By comparison, cross-linking of branched AP with either AM or another unit of AP

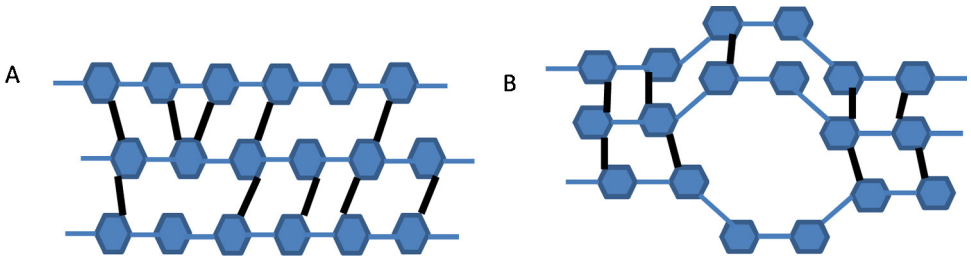

Scheme 2. Molecular structure of linear and branched polysaccharides cross-linked with epichlorohydrin (dark line segment): (A) cross-linked linear amylose and (B) cross-linked branched amylopectin.

Table 4
Equilibrium swelling properties in water (S_w) and in ethanol (S_e) of polysaccharides and PS–EPI copolymers at 295 K.

Copolymer	S_w (%)[1]	S_e (%)[1]
SSE	35 ± 4	8 ± 3
SSE-1	67 ± 12	13 ± 7
SSE-2	117 ± 18	27 ± 3
SSE-3	157 ± 21	8 ± 2
CSE	81 ± 8	13 ± 4
CSE-1	235 ± 9	8 ± 3
CSE-2	269 ± 6	8 ± 4
CSE-3	156 ± 11	1 ± 0.2
MSE	25 ± 5	4 ± 2
MSE-1	52 ± 7	4 ± 1
MSE-2	107 ± 9	3 ± 2
MSE-3	153 ± 9	2 ± 0.5
AMCSE	63 ± 7	1 ± 0.3
AMCSE-1	188 ± 11	2 ± 1
AMCSE-2	307 ± 16	18 ± 4
AMCSE-3	248 ± 12	14 ± 6
CE	166 ± 9	2 ± 0.1
CE-1	244 ± 11	120 ± 14
CE-2	205 ± 9	92 ± 8
CE-3	161 ± 3	15 ± 5

Note. Errors represent standard deviations from triplicate measurements.

is expected to result in more pronounced pore domains due to the effects of polysaccharide branching. Comparison of the polymers obtained from a common polysaccharide starting material (i.e. CSE1, CSE2 and CSE3) with variable cross-linking display variable water swelling. In the case of copolymers with similar cross-linking (CSE1 and CSE2), the water swelling capacity is lower relative to CSE3. There is no clear correlation between the degree of cross-linking and the swelling properties of the other polymer materials. However, there is a trend in the level of swelling of polymers with different AP and AM content. The results reveal that AMCSE has the highest swelling capacity in water; whereas, MSE show the lowest water swelling capacity, in agreement with a previous report (Ayoub & Rizvi, 2009). The results indicate that copolymers with high AM content adsorb more water than copolymers with high AP content.

3.6. Nitrogen gas adsorption

Molecular nitrogen is one of the most common gas adsorbates employed for the study of the textural parameters of adsorbent materials because of the ready availability of nitrogen, low cost, and its inert nature (Ghosh Dastidar & Netravali, 2013). Eq. (4) describes the relationship between the equilibrium amount of adsorbed nitrogen (n^o) onto the sorbent material against an external pressure (p) at constant temperature (T):

$$n^o = f\left(\frac{p}{p^o}\right)_{T,\ \text{gas, solid}} \quad (4)$$

where n^o is a function of the relative equilibrium gas pressure and the saturated vapor pressure (p^o) for the solid–gas adsorption process at isothermal conditions. In addition to nitrogen adsorption, dye-based methods (vide infra) have been used to provide complementary estimates of the textural properties of copolymer materials. Adsorptive dye probes such as *p*-nitrophenol (PNP) are suitable probe for the estimation of the surface area and pore structure (cf. Schemes 1 and 2) of polysaccharide adsorbents in aqueous solution, as described elsewhere (Mohamed, Wilson, & Headley, 2011).

In comparison to SSE1 (not shown), MSE1 (cf. Fig. 4A) shows low uptake of nitrogen up to a relative pressure (p/p^o) of 0.5. At values of $p/p^o > 0.5$, the copolymer displays an apparent negative nitrogen adsorption. At $p/p^o \sim 0.9$, greater adsorption of nitrogen occurs due to adsorption at the grain boundaries of the material. The slight negative oscillations are not due to leakage within the system because there is convergence between the adsorption and desorption at $p/p^o \sim 0$. The negative volume oscillation is attributed to shrinkage of the MSE-1 copolymer framework at low relative pressures and expansion of the framework at higher relative pressures due to pore filling of the adsorption sites (cf. Scheme 2) with nitrogen. This behavior has been observed previously in other copolymer systems (Ayoub & Rizvi, 2009). A comparison of the cellulose–EPI and starch–EPI copolymers suggests that the structure of cellulose–EPI is more rigid than the starch–EPI copolymer, in agreement with the well-defined mesopore characteristics of cellulose (Julkapli, Ahmad, & Akil, 2010).

3.7. Adsorption of PNP in aqueous solution

Fig. 5 shows 3-D plots representing the percent uptake of PNP from aqueous solution by the polysaccharides and PS–EPI copolymers at 298 K and pH 6. In all cases, a fixed concentration of dye and dosage of adsorbent was used throughout, as indicated. A comparison of panels A-C for copolymers with the same EPI content shows that the level of PNP removal increases as the concentration of PNP increases. This is true for most of the PS–EPI copolymers but some exceptions were observed for SSE and CSE, where the level of dye uptake decreased for various concentrations of PNP; from 0.1 to 10 mM or from 10 to 25 mM. The results suggest that SSE and CSE have fewer adsorption sites compared to the other copolymers which may be understood according to difference in surface chemistry and textural properties (cf. Schemes 1 and 2). According to panels B and C, the sorption capacities for PNP does not follow a trend for polymers that possess an irregular or non-uniform morphology. In Fig. 5 A, polymers with high amylose (AM PS–EPI) display decreased sorption as the EPI ratio increased, whereas; high amylopectin (AP) copolymers display high PNP sorption as the EPI ratio is increased. The decrease in PNP sorption capacity in the case of AMCSE copolymers is attributed to greater cross-linking between AMCSE chains. This results in smaller micropore structures which hinder access of PNP to the adsorption sites. On the other hand, greater cross-linking of the MSE-EPI copolymers does not yield micropore structures, due to branching of AMCSE-EPI polymers that may serve as suitable binding sites for PNP.

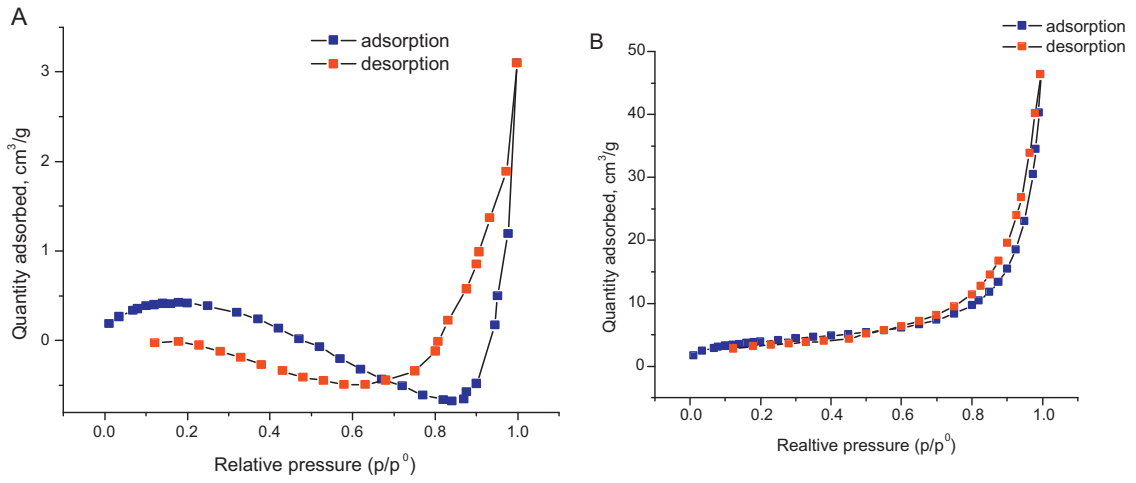

Fig. 4. Nitrogen adsorption–desorption isotherms: (A) MSE1 and (B) cellulose at 77 K.

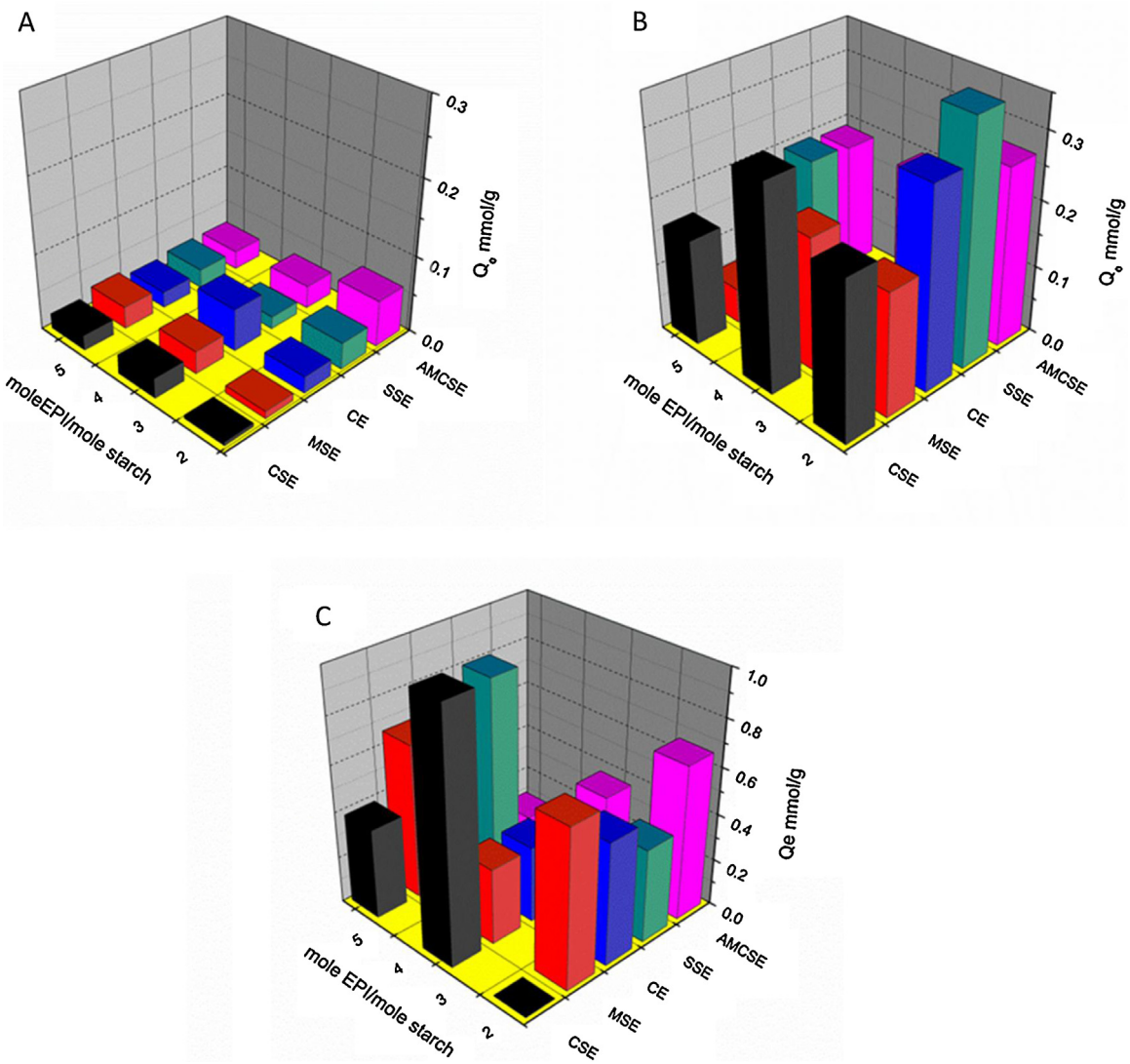

Fig. 5. Sorptive uptake of PNP by native polysaccharides and their cross-linked forms at variable dye concentration at pH 6 and 295 K: (A) C_0 = 0.1 mM PNP, (B) C_0 = 10 mM PNP, and (C) C_0 = 25 mM PNP. Panels A and B are scaled along the same *z*-axis range for comparative purposes.

The effect of matching between the pore size and the guest size was evidenced by an increased adsorption capacity by Huang, Yan, and Huang (2009). They report a water-compatible hyper cross-linked polystyrene type resin to adsorb PNP where matching of the pore size relates to the dimensions of PNP. Higher levels of cross-linking may contribute negative steric effects for the uptake of PNP; whereas, intermediate cross-linking does not. The variation in sorptive uptake observed for the intermediate cross-linked copolymers may reflect the importance of surface chemistry, as noted in other related studies (Mohamed et al., 2010; Mohamed, Wilson, Headley, & Peru, 2011).

4. Conclusion

In this study, a series of polymers were prepared by cross-linking different polysaccharides (PS) of variable composition (i.e. amylose, amylopectin, and cellulose) with epichlorohydrin. Cross-linking was carried out at different relative composition at an optimal temperature of 50 °C to afford PS–EPI polymers with favorable adsorption properties toward nitrogen gas, solvents (i.e. water and ethanol), and *p*-nitrophenol in aqueous solution at pH 6. Copolymers with high AM content have relatively high adsorption capacity for water. Variable dye sorption of polymers at comparable cross-link density reflect differences in the surface properties related to the accessibility of dipolar functional groups (—OH) on the polymer surface. Further studies are underway to ascertain the specific structural role of the polymer structure and its dependence on the sorptive properties with various adsorbates.

Acknowledgments

The authors gratefully acknowledge the support for this research provided by the Government of Saskatchewan through the generous support of the Agriculture Development Fund (PROJECT #: 20110162) and the University of Saskatchewan.

Appendix A. Supplementary data

Supplementary data associated with this article can be found, in the online version, at http://dx.doi.org/10.1016/j.carbpol.2014.06.083.

References

Ashish, P., Khanderao, J., & Deelip, D. (2013). Cross linked high amylose starch biodegradable implants for sustained delivery of ciprofloxacin hydrochloride. *International Journal of Pharmacy and Pharmaceutical Sciences*, *5*, 391–397.

Ayoub, A. S., & Rizvi, S. S. H. (2009). An overview on the technology of cross-linking of starch for nonfood applications. *Journal of Plastic Film and Sheeting*, *25*, 25–45.

Azubuike, C., & Okhamafe, A. (2012). Physicochemical, spectroscopic and thermal properties of microcrystalline cellulose derived from corn cobs. *International Journal of Recycling of Organic Waste in Agriculture*, *1*, 1–7.

Broekhoff, J. C. P., & De Boer, J. H. (1968). Studies on pore systems in catalysts: XI. Pore distribution calculations from the adsorption branch of a nitrogen adsorption isotherm in the case of ink-bottle type pores. *Journal of Catalysis*, *10*, 153–165.

Copeland, L., Blazek, J., Salman, H., & Tang, M. C. (2009). Form and functionality of starch. *Food Hydrocolloids*, *23*, 1527–1534.

Crini, G. (2005). Recent developments in polysaccharide-based materials used as adsorbents in wastewater treatment. *Progress in Polymer Science*, *30*, 38–70.

da Sil Va, P. M. S., Oliveira, J. C., & Rao, M. A. (1997). Granule size distribution and rheological behavior of heated modified waxy and unmodified maize starch dispersions. *Journal of Texture Studies*, *28*, 123–138.

Delval, F., Vebrel, J., Morcellet, M., & Crini, G. (2000). Sorption properties toward aromatic compounds of insoluble crosslinked polymers containing starch derivatives. *Progress in Polymer Science*, *5*, 137–143.

Delval, F., Crini, G., Bertini, S., Filiatre, C., & Torri, G. (2005). Preparation, characterization and sorption properties of crosslinked starch-based exchangers. *Carbohydrate Polymers*, *60*, 67–75.

Ghosh Dastidar, T., & Netravali, A. (2013). Cross-linked waxy maize starch-based green composites. *ACS Sustainable Chemistry & Engineering*, *12*, 1537–1544.

Gomes, M. E., Ribeiro, A. S., Malafaya, P. B., Reis, R. L., & Cunha, A. M. (2001). A new approach based on injection moulding to produce biodegradable starch-based polymeric scaffolds: Morphology, mechanical and degradation behaviour. *Biomaterials*, *22*, 883–889.

Hamdi, G., Ponchel, G., & Duchêne, D. (2001). Formulation of epichlorohydrin cross-linked starch microspheres. *Journal of Microencapsulation*, *18*, 373–383.

Huang, J., Yan, C., & Huang, K. (2009). Removal of p-nitrophenol by a water-compatible hypercrosslinked resin functionalized with formaldehyde carbonyl groups and XAD-4 in aqueous solution: A comparative study. *Journal of Colloid and Interface Science*, *332*, 60–64.

Julkapli, N. M., Ahmad, Z., & Akil, H. M. (2010). X-ray diffraction studies of cross linked chitosan with different cross linking agents for waste water treatment application. *AIP Conference Proceedings*, *1202*, 106–111.

Kamm, B., & Kamm, M. (2004). Principles of Biorefineries. *Applied Microbiology and Biotechnology*, *64*, 137–145.

Kaur, B., Ariffin, F., Bhat, R., & Karim, A. A. (2012). Progress in starch modification in the last decade. *Food Hydrocolloids*, *26*, 398–404.

Kubo, A., Akdogan, G., Nakaya, M., Shojo, A., Suzuki, S. H., Satoh, H., et al. (2010). Structure, physical, and digestive properties of starch from wx ae double-mutant rice. *Journal of Agricultural and Food Chemistry*, *58*, 4463–4469.

Kyzas, G. Z., Bikiaris, D. N., & Lazaridis, N. K. (2008). Low-swelling chitosan derivatives as biosorbents for basic dyes. *Langmuir*, *24*, 4791–4799.

Marques, A. P., Reis, R. L., & Hunt, J. A. (2002). The biocompatibility of novel starch-based polymers and composites: In vitro studies. *Biomaterials*, *23*, 1471–1478.

Mohamed, M. H., Wilson, L. D., & Headley, J. V. (2010). Estimation of surface accessibility of β-cyclodextrin in cyclodextrin-copolymer materials. *Carbohydrate Polymers*, *80*, 186–196.

Mohamed, M. H., Wilson, L. D., & Headley, J. V. (2011). Surface area and pore structure properties of urethane-based copolymers containing β-cyclodextrin. *Journal of Colloid and Interface Science*, *357*, 215–222.

Mohamed, M. H., Wilson, L. D., Headley, J. V., & Peru, K. M. (2011). Investigation of the sorption properties of β-cyclodextrin-based polyurethanes with phenolic dyes and naphthenates. *Journal of Colloid and Interface Science*, *356*, 217–226.

Onofre, F. O., & Wang, Y. J. (2010). Sustained release properties of crosslinked and substituted starches. *Journal of Applied Polymer Science*, *117*, 1558–1565.

Pratt, D. Y., Wilson, L. D., Kozinski, J. A., & Mohart, A. M. (2010). Preparation and sorption studies of β-cyclodextrin/epichlorohydrin copolymers. *Journal of Applied Polymer Science*, *116*, 2982–2989.

Richardson, S., & Gorton, L. (2003). Characterisation of the substituent distribution in starch and cellulose derivatives. *Analytica Chimica Acta*, *497*, 27–65.

Sandra, K. (2009). *Polysaccharide materials performance by design*. American Chemical Society.

Sasaki, T., & Matsuki, J. (1998). Effect of wheat starch structure on swelling power. *Cereal Chemistry Journal*, *75*, 525–529.

Scheller, J., & Conrad, U. (2005). Plant-based material, protein and biodegradable plastic. *Current Opinion in Plant Biology*, *8*, 188–196.

Šimkovic, I., & Jakab, E. (2001). Thermogravimetry/mass spectrometry study of weakly basic starch-based ion exchanger. *Carbohydrate Polymers*, *45*, 53–59.

Šimkovic, I., Laszlo, J. A., & Thompson, A. R. (1996). Preparation of a weakly basic ion exchanger by crosslinking starch with epichlorohydrin in the presence of NH_4OH. *Carbohydrate Polymers*, *30*, 25–30.

Singh, N., Singh, J., Kaur, L., Singh Sodhi, N., & Singh Gill, B. (2003). Morphological, thermal and rheological properties of starches from different botanical sources. *Food Chemistry*, *81*, 219–231.

Tester, R. F., & Morrison, W. R. (1990). Swelling and gelatinization of cereal starches. I. Effects of amylopectin, amylose, and lipids. *Cereal Chemistry*, *67*, 551–557.

Tian, Y., Zhu, Y., Bashari, M., Hu, X., Xueming, X., & Zhengyu, J. (2013). Identification and releasing characteristics of high-amylose corn starch-cinnamaldehyde inclusion complex prepared using ultrasound treatment. *Carbohydrate Polymers*, *91*, 586–589.

Varum, K. M., & Smidsrod, O. (2005). *Polysaccharides – Structure and diversity and functional versatility*. New York: Marcel and Dekker.

Xie, F., Yu, L., Su, B., Liu, P., Wang, J., Hongshen, L., et al. (2009). Rheological properties of starches with different amylose/amylopectin ratios. *Journal of Cereal Science*, *49*, 371–377.